ADVANCING EARTH AND SPACE SCIENCES

JGR Earth Surface

RESEARCH ARTICLE
10.1029/2024JF007950

Key Points:

- Resistance to sheet and lateral erosion was uncorrelated and depended on the thickness of the cohesive topsoil accreted by marsh vegetation
- Back-barrier marshes had thin cohesive topsoils and sandy subsoils leading to sheet erosion resistance but vulnerability to lateral erosion
- Soft engineering may increase back-barrier island's soil erosion resistance by creating sheltered conditions for marsh development

Supporting Information:

Supporting Information may be found in the online version of this article.

Correspondence to:

B. Marin-Diaz,
bea.marin.diaz@gmail.com

Citation:

Marin-Diaz, B., Reijers, V. C., Meijer, L., van der Wal, D., Olff, H., Bouma, T. J., & Govers, L. L. (2025). Quantifying soil resistance to sheet and lateral erosion across different habitats on a managed sandy back-barrier island. *Journal of Geophysical Research: Earth Surface*, *130*, e2024JF007950. https://doi.org/10.1029/2024JF007950

Received 19 JUL 2024
Accepted 20 MAY 2025

Author Contributions:

Conceptualization: Beatriz Marin-Diaz, Valérie C. Reijers, Daphne van der Wal, Han Olff, Tjeerd J. Bouma, Laura L. Govers
Data curation: Beatriz Marin-Diaz, Linda Meijer
Formal analysis: Beatriz Marin-Diaz, Han Olff
Investigation: Beatriz Marin-Diaz, Valérie C. Reijers, Linda Meijer, Daphne van der Wal, Han Olff, Tjeerd J. Bouma, Laura L. Govers
Methodology: Beatriz Marin-Diaz, Daphne van der Wal, Han Olff, Tjeerd J. Bouma, Laura L. Govers

Quantifying Soil Resistance to Sheet and Lateral Erosion Across Different Habitats on a Managed Sandy Back-Barrier Island

Beatriz Marin-Diaz[1,2,3], Valérie C. Reijers[4,5], Linda Meijer[6], Daphne van der Wal[1,7], Han Olff[2], Tjeerd J. Bouma[1,2,4], and Laura L. Govers[2,5]

[1]Department of Estuarine and Delta Systems, NIOZ Royal Netherlands Institute for Sea Research, Yerseke, the Netherlands, [2]Conservation Ecology Group, Groningen Institute for Evolutionary Life Sciences, University of Groningen, Groningen, the Netherlands, [3]Department of Environmental Engineering Sciences, University of Florida, Gainesville, FL, USA, [4]Department of Physical Geography, Faculty of Geosciences, Utrecht University, Utrecht, The Netherlands, [5]Department Coastal Systems, NIOZ Royal Netherlands Institute of Sea Research, Den Burg, The Netherlands, [6]Aquatic Ecology and Water Quality Management Group, Wageningen University & Research, Wageningen, The Netherlands, [7]Faculty of Geo-Information Science and Earth Observation (ITC), University of Twente, Enschede, The Netherlands

Abstract Back-barrier islands are understudied, dynamic, soft-sediment coastal landscapes located in fetch-limited environments. They are of key ecological importance; however, they are threatened by global change impacts including increasing storm surges and sea level rise. This study aimed to investigate the soil erosion resistance to hydraulic forces of different habitats across a sandy back-barrier island with characteristic sandy subsoils that has been managed >100 years to prevent its complete erosion and submergence. We quantified sheet and lateral soil erosion resistance in flumes, investigated their correlations with sediment and belowground vegetation characteristics, and discussed how these characteristics may relate to the island's past management and development. Soil cores were collected from the barrier dune ridge, back-barrier marshes and unvegetated sandflats and were exposed laterally to waves (lateral erosion) and horizontally to water flow (sheet erosion). Resistance to sheet and lateral erosion was not correlated. Resistance to lateral erosion depended on the thickness of the cohesive topsoil layer accreted by the marsh vegetation on top of a sandy subsoil. For instance, marsh soils with thin cohesive topsoils were resistant to sheet erosion (<0.5 cm erosion in 3 hr) but not to lateral erosion (collapsed within the first 10 min), which could make them vulnerable to wave attacks if they get laterally exposed during island erosion. Topsoil thickness was related to marsh elevation and age. In turn, the development of the cohesive layer may be related to the past management of the island, as soft engineering measures such as beach nourishments can create sheltered conditions for marsh development.

Plain Language Summary Back-barrier islands are features of sandy coastal landscapes that can be found in the shelter of barrier island chains. They have high ecological value as coastal breeding bird habitats or roosting sites for migratory birds. They are however threatened by sea level rise and increasing storm surges due to climate change. We quantified how soil and plant properties on a back-barrier island affect soil erosion resistance. We found that the thickness of the fine-grained top layer trapped by salt marsh plants positively improved the erosion resistance of both the topsoils and sediment cliffs. The thickness of this erosion-resistant layer was determined by marsh age and elevation. Management strategies to prevent climate change-induced erosion of back-barrier islands may increase the island's soil erosion resistance by creating (long lasting) sheltered conditions for marsh development.

1. Introduction

Barrier islands are dynamic, migrating, soft-sediment coastal landscapes that play a major role in flood defense by protecting mainland shorelines from ocean waves and storms (Cooper et al., 2007; Oertel, 1985; Otvos, 2020). Back-barrier islands or fetch-limited barrier islands are a type of smaller sandy barrier island that can be found behind the ocean barrier islands in estuaries or bays (Cooper et al., 2007). These islands are of key ecological importance in estuarine coastal landscapes by providing breeding and roosting habitat for shore birds (Loonstra et al., 2016; Piersma et al., 1993) and pupping ground for gray seals (Brasseur et al., 2015). In contrast to ocean barrier islands, back-barrier islands do not often accommodate aeolian-formed dunes. Instead, a beach or a chenier ridge can be found on the exposed seaward side created by shells and beach wrack deposited during

Visualization: Beatriz Marin-Diaz
Writing – original draft: Beatriz Marin-Diaz
Writing – review & editing: Beatriz Marin-Diaz, Valérie C. Reijers, Linda Meijer, Daphne van der Wal, Han Olff, Tjeerd J. Bouma, Laura L. Govers

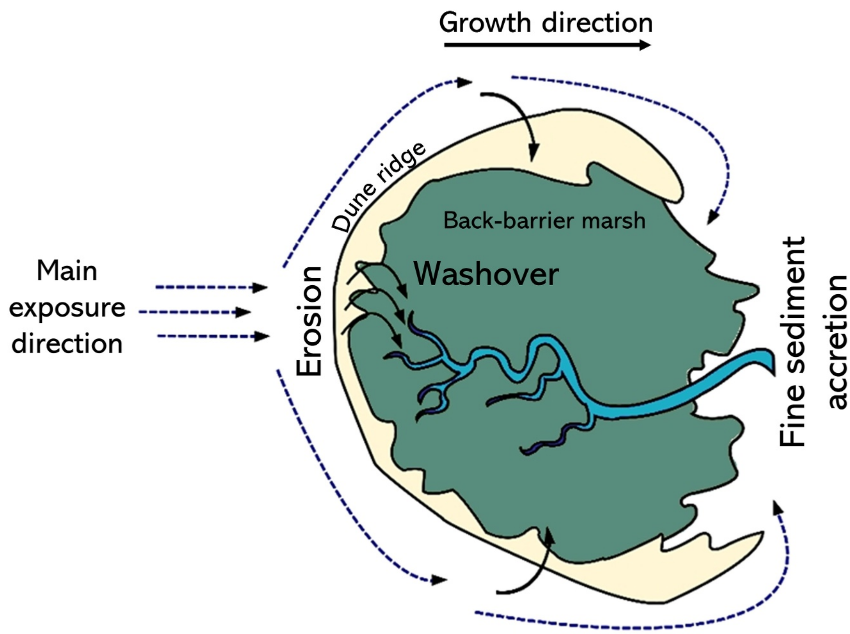

Figure 1. Processes important for the formation and dynamics of small back-barrier islands. The barrier ridge is eroded during storms on the exposed side while the back-barrier marsh grows during calmer storm conditions. Dashed arrows indicate directions of sediment transport. Illustration modified from Govers and Reijers (2021).

stochastic storm surges (Castagno et al., 2018; McBride et al., 2007; Neal et al., 2002; Nordstrom & Jackson, 2012; Pilkey et al., 2009; Sirianni et al., 2022) (Figure 1). During storms, islands can both accrete through overwash processes and erode, especially around the island edges (Castagno et al., 2018; Conery et al., 2018; Otvos, 2020; Sirianni et al., 2022; Timmons et al., 2010) (Figure 1). Additionally, the chenier may migrate over the marsh, promoting marsh development in the new sheltered area while leaving a marsh fringe on the exposed side of the island (Cooper, 2013).

The shape and migration of back-barrier islands are not only dependent on storms but also on vegetation characteristics (Cooper et al., 2007; Morton, 2002; Pilkey et al., 2009). Coastal vegetation may play a key role in stabilizing back-barrier islands by attenuating waves, winds and currents (Feagin et al., 2015; Pilkey et al., 2009). In addition, vegetation traps fine sediment, accumulates organic matter and produces belowground biomass (i.e., roots and rhizomes), all variables related to higher erosion resistance (e.g., dunes: De Battisti et al., 2020; marshes: Feagin et al., 2009; Ford et al., 2016; Marin-Diaz, Govers, et al., 2021; Marin-Diaz et al., 2022; Spencer et al., 2016; Wang et al., 2017). High root density is especially important for erosion reduction in sandy soils for both lateral erosion (De Battisti et al., 2019; Lo et al., 2017; Marin-Diaz, Govers, et al., 2021) and topsoil erosion (Marin-Diaz et al., 2022). Therefore, vegetation-mediated soil modifications may be an important factor for predicting island development and resistance to storm surges. However, to our knowledge, soil erosion-resistance of different habitats in back-barrier islands in relation to island developmental stage and management has never been investigated.

Sheet erosion (i.e., topsoil erosion) can occur due to increased bed shear stress from currents or waves during storms (Van Rijn, 1984a, 1984b), and is an integral component of storm surge and overwash processes (Figure 1). Lateral erosion, also called cliff erosion, may be important during storm surges in zones laterally exposed to waves such as the island edges (Leonardi et al., 2018). Back-barrier marshes that were initially on interior areas of barrier islands may become exposed due to the faster migration of the dune or chenier over the marsh (Cooper, 2013). Furthermore, back-barrier marshes, where cohesive topsoils can form on initially unstable sand flats during marsh development, may have sandy subsoils which are typically non-cohesive (Marin-Diaz, Govers, et al., 2021; Olff et al., 1997). This suggests that if these types of marsh profiles become exposed on the island edges due to island erosion, they could be vulnerable to lateral erosion even if they are resistant to sheet erosion. However, to our knowledge, simultaneous investigation of sheet and lateral soil erosion resistance has not been previously conducted, and this is especially important for sandy marshes.

Deterioration of barrier islands due to sea level rise and extreme storm surges (Seneviratne et al., 2021), changes in hydrodynamics (e.g., by building of dams), changes in sediment supply or human inhabitation (Conery et al., 2018; Govers & Reijers, 2021; Morton, 2002; Otvos, 2020; Timmons et al., 2010) may lead to the need for management measures to prevent their complete loss (Oliver & Ramirez-Avila, 2019; Rosati, 2009). Soft engineering measures that promote vegetation-sedimentation feedback or the construction of chenier-like dikes can promote island integrity and hence enhance their stability. For example, the construction of elevated landforms such as sand dikes create more sheltered conditions on the wake of the island, which may induce marsh formation (Govers & Reijers, 2021). In some cases, reinforcement may be required as the island ecosystem might erode completely, which may be undesirable from the perspective of human use or key ecosystem functions. On the other hand, the migration of back-barrier islands is a natural process in which dynamic processes forming these islands (e.g., storm surges) promote high habitat heterogeneity and vegetation-sedimentation processes (Cooper et al., 2007; Osswald et al., 2019; Rosati, 2009). Reducing morphological dynamics due to denser or more stable vegetation may thus affect the ecosystem functioning of these islands (Osswald et al., 2019; Rosati, 2009). Overall, most of the research on barrier island management focuses on ocean barrier islands (Oliver & Ramirez-Avila, 2019; Rosati, 2009) and to our knowledge, no studies have focused on the effects of soft engineering measures on back-barrier islands yet.

To further understand the soil erosion resistance of sandy back-barrier islands with characteristic sandy subsoils, this study (a) quantified sheet and lateral soil erosion resistance of different habitats across a managed sandy back-barrier island, (b) investigated correlations between sheet and lateral soil erosion resistance in relation to sediment and belowground vegetation characteristics, and (c) explored how these characteristics may be related to the past management and development of the island. We focused on small-scale sediment erosion to assess specific processes, with island-scale erosion rates, which involve other large-scale factors, being beyond the scope of this study.

2. Materials and Methods

2.1. Description of the Study Site and Past Management

The study was conducted on Griend, an uninhabited back-barrier island in the Dutch Wadden Sea (53°14′25″N, 5°14′54″E) (Figures 2a and 2b). The normal tidal range in this area is ∼1.9 m, with a mean high tide level of ∼0.83 m MSL (mean sea level) and a mean spring high tide level of ∼0.93 m MSL (RWS, 2013). The closest hydrodynamic data to the island was found in a paper by Marin-Diaz, Fivash, et al. (2021), which recorded wave data between 2017 and 2019 on the tidal flat south of Griend at an elevation of approximately −0.3 m MSL. The measured maximum mean water depths reached approximately 2 m MSL, and the highest significant wave height during high tides was ∼0.7 m, although most of the significant wave heights were below 0.2 m.

In this region, the formation of barrier islands started on an initial coarse-grained sandy substrate, and once the back-barrier marsh vegetation was established, a layer of fine-grained sediment and organic matter started accreting over time on top of the sand (Olff et al., 1997). Similarly, Griend is characterized by sandy soils, with a distinguishable thin layer of cohesive fine-grained sediment accreted on top of the sand by the marsh vegetation in the back-barrier marsh area (Figures 2c and 2d).

Back-barrier islands are mobile but can disappear due to changes in hydrodynamics and sediment dynamics in the tidal basin (Govers & Reijers, 2021). In 1930, the adjacent basin (now Lake Ijssel) was closed off by a 30 km long dam ("Afsluitdijk") (Figure 2a), resulting in a reported increase in the tidal amplitude (∼15 cm or more) and storm surge levels in the area around Griend (Brouwer et al., 1950; Govers & Reijers, 2021). Although exact values of this change around Griend are not available, an increase in the tidal range of ∼0.5 m was measured in the nearby location of Harlingen (Rietveld, 1962). This alteration led to a trend toward gradual disappearance of the island (Brouwer et al., 1950; Govers & Reijers, 2021) (Figure 3a). To prevent complete disappearance of the island, and the consequent loss of its key function as a bird sanctuary (Loonstra et al., 2016; Piersma et al., 1993) and pupping ground for gray seals (Brasseur et al., 2015), several large-scale management interventions including various types of breakwaters and dikes have taken place since 1925 (Govers & Reijers, 2021). In the 1980s (1985–1988), a 2.5 km long sand dike with a hook shape was constructed on the west and north sides of the island (900,000 m^3 sand) to prevent further erosion (Figures 3a and 3b). Subsequently, this measure led to marsh development in the sheltered region between the dune ridges, which continued growing toward the east. In 2016, the western side of the dike had almost disappeared, and a large (200,000 m^3) beach nourishment on the western side of the island

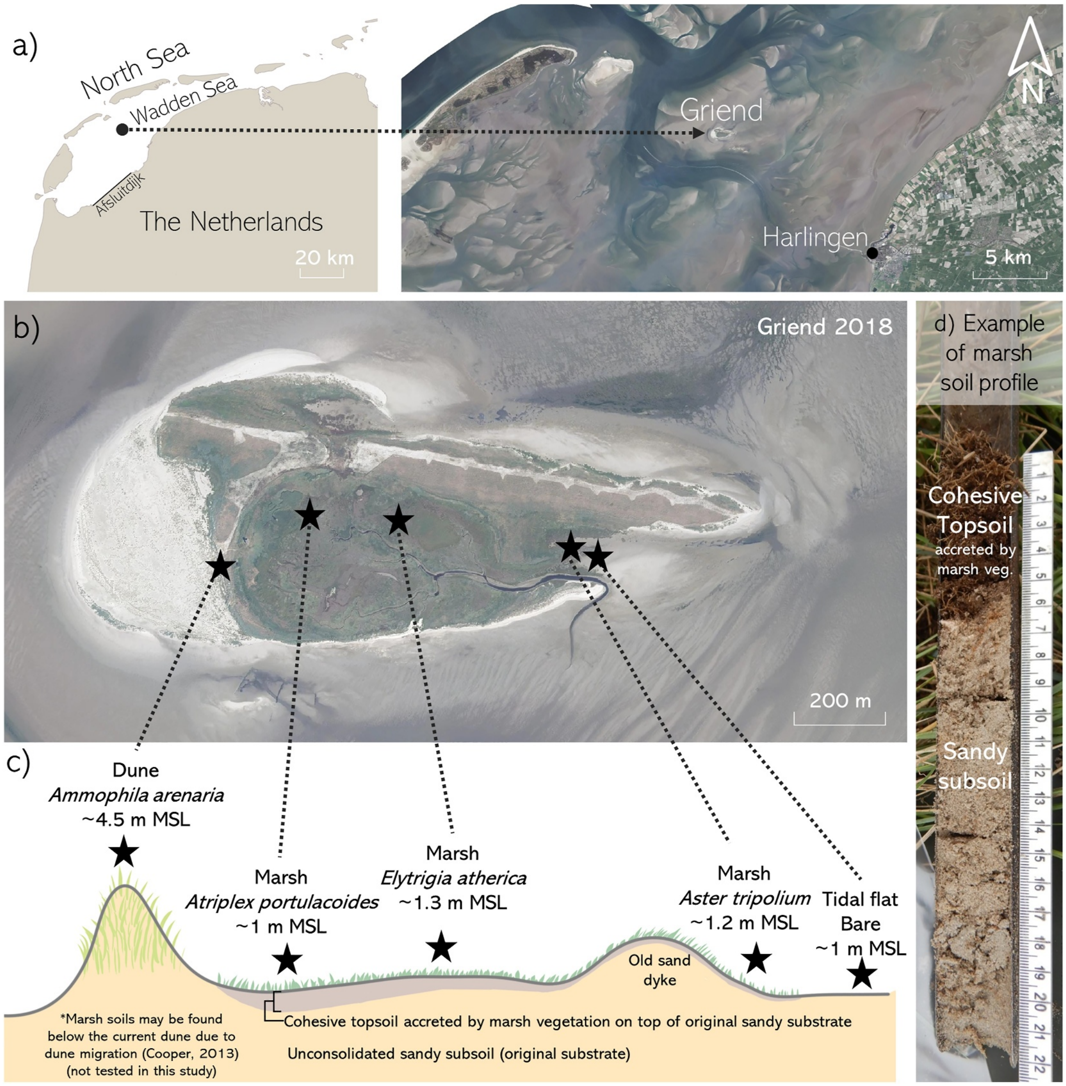

Figure 2. (a) Location of the fetch-limited back-barrier island of Griend in the Netherlands; (b) Locations of the sampling sites in Griend; (c) Schematic representation of the island profile depicting sandy subsoils and cohesive topsoil accreted by the back-barrier marsh. Stars indicate the approximate location of the sampling sites and the elevation measured in the field (Mean Sea Level); (d) Example of a marsh soil profile where the cohesive top layer can be differentiated from the sandy subsoil (ruler in cm). Aerial imagery source: PDOK (Dutch Public Geodata Portal).

was implemented. Additional actions such as the construction of shell ridges (20,000 m^3), sod removal to set back vegetation development on the dike/dune and a washover to mimic natural inundation dynamics of the island were also performed (Govers & Reijers, 2021). These interventions led to the present island shape with a relatively young marsh (Figures 3a and 3b). The contours of the island in Figure 3a were manually delineated by tracing the shoreline from available aerial imagery (Google Earth).

2.2. Sheet and Lateral Erosion

Soil cores were collected in March 2019, in five locations along a cross section of the island, to test the resistance to sheet and lateral erosion with different vegetation and soil types. From west to east, three cores for sheet erosion and three cores for lateral erosion were collected on each sampling location (Figures 2b and 2c): in the dunes dominated by *Ammophila arenaria* (~4.5 m MSL) followed by the oldest marsh dominated by *Atriplex portulacoides* (~1 m MSL), marsh dominated by *Elytrigia atherica* (~1.3 m MSL), marsh dominated by *Aster tripolium* (~1.2 m NAP) and finally, bare tidal flat (~1 m MSL). The elevation of each sampling site was measured

10.1029/2024JF007950

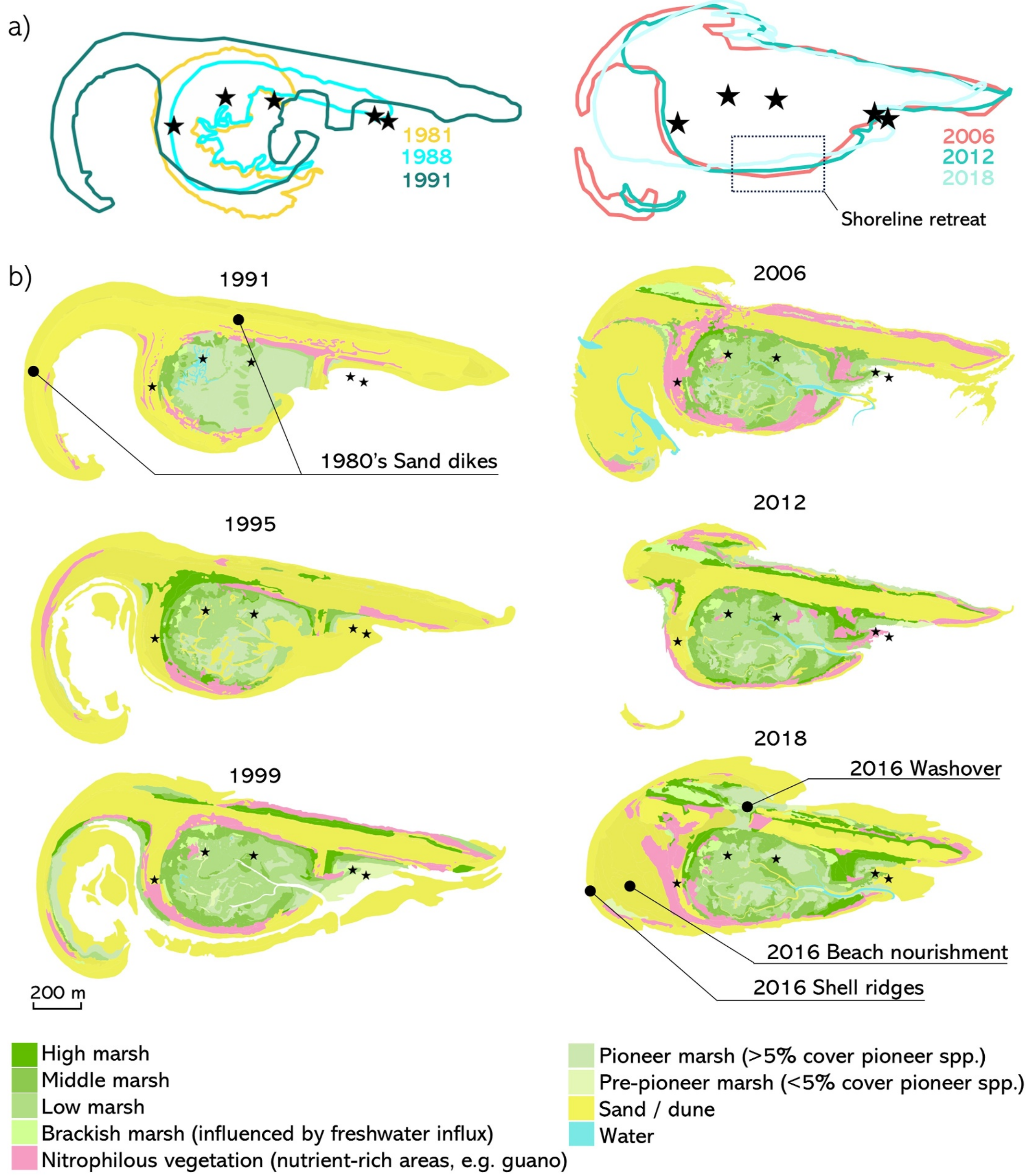

Figure 3. (a) Development of the island between 1981 and 2018. Contours were manually delineated by tracing the shoreline from available aerial imagery (Google Earth) in designated years; and (b) Evolution of the island and its habitats over the years, including the main soft engineering measures performed. Habitat polygon maps were obtained from the VEGWAD program (Rijkswaterstaat). Stars indicate the sampling locations.

using an RTK-GPS (Leica GS12). All soil cores were transported to the Royal Netherlands Institute for Sea Research (NIOZ) in Yerseke and stored for 1 week in tanks with seawater from the Oosterschelde estuary until the erosion test. The duration of the erosion tests was not set to mimic a real storm or calculate island-scale erosion rates, but to reach constant erosion rates and test differences in erosion resistances between different habitats, using conditions comparable to previous studies from Lo et al. (2017), Wang et al. (2017), Marin-Diaz, Govers, et al. (2021) and Marin-Diaz et al. (2022).

Sheet erosion was determined in a fast-flow flume developed at the NIOZ as in Marin-Diaz et al. (2022). The flume included a water tank that was filled at a constant flow rate of 247 L/min. The tank had an opening at the bottom of one corner, measuring 2.4 cm in height and 11 cm in width, from which water flowed at a constant speed of 2.3 m/s and with an estimated bottom shear stress of approximately 27 N/m^2, which could occur for example, during a dike breach (see calculations in Appendix S1 of Marin-Diaz et al., 2022). The outflowing water was disposed of. The samples for sheet erosion tests consisted of rectangular soil cores of 40 cm long × 20 cm high × 12 cm width. The cores were extracted with a custom-made steel box core with sharp edges that cut through roots and rhizomes. Next, they were placed into a customized wooden box, which fitted in the fast-flow flume. The soil cores were then cut to 32 cm in length, with the remaining part used for belowground vegetation analysis. Aboveground vegetation was clipped before the erosion test to focus on the intrinsic soil erosion independent of the effect of the aboveground vegetation as in Marin-Diaz et al. (2022). The samples in the wooden boxes were placed on the other side of the flume opening and exposed to continuous water flow. Topsoil erosion was determined after 10 min, 1, 2, and 3 hr as the average change in elevation measured with a calibrated stick in a spatial grid of 3 cm in the axis parallel to the flow and 3.7 cm in the axis cross-stream, with a 1 mm vertical resolution.

Lateral erosion was determined in four wave flumes developed at the NIOZ of 360 cm long × 90 cm high × 82 cm wide as in Lo et al. (2017), Wang et al. (2017), and Marin-Diaz, Govers, et al. (2021). The same settings of ∼8 cm wave height with swash intersecting the whole core were used as in Lo et al. (2017) and Marin-Diaz, Govers, et al. (2021). Lateral erosion samples consisted of round soil cores of 15 cm diameter and 20 cm depth collected by inserting PVC pipes with sharp edges that cut through roots and rhizomes in the soil and carefully digging them out as in Marin-Diaz, Govers, et al. (2021). The cores were transferred into metal cylinders with 12 cm width opening in the longitudinal side. The exposed side was cleanly sliced and adjusted to 15 cm height. Lateral erosion was determined after 10 min, 1, 2, 4, 8, 24, 32, and 45 hr of wave exposure. Cores with readily erodible sandy bottom collapsed after 10 min, and only the marsh cores dominated by *Atriplex* resisted for the entire 45 hr. Erosion (% of volume eroded) was determined by photogrammetry (structure from motion) (Marin-Diaz, Govers, et al., 2021; Nieuwhof et al., 2015).

2.3. Belowground Vegetation Properties

Belowground biomass from the subsample of the topsoil erosion core was cleaned over a 1 mm sieve and separated into roots and rhizomes as in (Marin-Diaz, Govers, et al., 2021). All the rhizomes, including those that were dead, were distinguishable and subsequently separated into the rhizome compartment. From each sample, a representative subsample of coarse roots (>0.5 mm diameter) and fine roots (<0.5 mm diameter) was separated from the root fraction to extrapolate the biomass of coarse roots and fine roots to the entire sample. Fine roots included some fine dead root material that could not be distinguished and removed (cf. De Battisti et al., 2019; Marin-Diaz, Govers, et al., 2021). Biomass was obtained by drying the samples at 60°C until constant weight. Compartmental densities were calculated as the dry biomass by the soil sample volume (g cm^{-3}). This biomass was representative of both sheet and lateral erosion core samples.

2.4. Sediment Properties

Sediment samples up to ∼30 cm depth were collected next to each erosion core with a sharp 2.2 cm diameter gouge that easily cuts through rhizomes and roots. We checked that the gouge did not cause compaction of the sample. If compaction was observed, the collection was repeated, and if needed, the superficial roots and rhizomes were carefully cut around the perimeter of the gouge to facilitate the insertion. A clear transition between the coarse sandy subsoil and the fine-grained cohesive topsoil allowed us to measure the thickness of the cohesive topsoil (Figure 2d) (Elschot et al., 2015; Olff et al., 1997). To further explore the depth of the cohesive top layer on the island, cohesive topsoil thickness was measured at 10 additional locations along the cross section of the island, and four perpendicular to the main transect. Sediment properties were determined from the top 5 cm of soil and from the sandy subsoil up to 20 cm, separately. For marsh cores with cohesive layers thinner than 5 cm, the properties of the top layer were determined up to the sandy subsoil to avoid mixing. Sediment samples were weighed and freeze-dried for 4 days. Water content was determined by subtracting dry weight from wet weight. Bulk density was calculated as the dry weight per known volume (g cm^{-3}). Soil organic content was measured by the loss on ignition method after burning the sediment for 6 hr at 450°C as in Lo et al. (2017). Thick rhizomes were removed to avoid biases in soil organic content. Sediment grain size was determined using a laser particle sizer (Malvern ® Mastersizer 2000). Lastly, a dynamic soil deformation test was conducted in the field, next to each erosion core, as a proxy for soil porosity and deformability by releasing a 5 kg weight of 10 cm diameter 10 times from 1.5 m height through a guiding PVC pipe directly into the soil. This method was adapted from

Howison et al. (2015) and utilized by Marin-Diaz et al. (2022). Dynamic soil deformation was the distance between the soil surface and the bottom of the compacted soil (cm).

2.5. Statistical Analysis

One-way ANOVAs followed by a Tukey's HSD post hoc tests were used to test differences on soil and vegetation properties among habitats. A one-way ANOVA followed by a Tukey's HSD post hoc test was used to test for differences in sheet erosion between the marsh habitats that resisted the erosion test (*Atriplex*, *Elytrigia* and *Aster*) using the erosion values at the end of the 3-hr erosion test. To avoid bias in the results, the erosion values after 10 min, which mainly consisted of loose debris, were subtracted from the total mean erosion after 3 hr. For lateral erosion, only marsh-*Atriplex* samples resisted, while all other treatments were completely eroded. As there was no variation for comparison, ANOVAs were not performed in this case; instead, descriptive statistics were provided. Model assumptions were tested with histograms and residual plots.

To examine how erosion resistance correlated with soil and vegetation properties, we performed a first analysis including all samples. This included samples that were either completely eroded in the first minutes of exposure or barely eroded after full exposure to the erosion tests (*Atriplex*, *Elytrigia*, and *Aster*). Due to the nature of the erosion results, a binomial distribution (either completely eroded or not eroded) was used to investigate the relationships between both types of erosion (sheet and lateral) and the belowground vegetation and soil variables. Logistic regression models, performed with Bayesian Generalized Linear Models (GLMs) with binomial distribution using the package *arm*, were used to model the probability of complete sheet erosion and complete lateral erosion in relation to vegetation and soil properties. Bayesian GLMs were performed to deal with the complete separation in the logistic regressions, which can occur when the predictor is perfectly predictive of the outcome (Gelman et al., 2008). The significance of the models was tested using a Type II Wald χ^2 test.

The second part of the analysis focused on the samples that resisted after the sheet erosion tests (*Atriplex*, *Elytrigia*, and *Aster*). Mean sheet erosion depth after the 3-hr erosion test corrected for the initial debris erosion (cm) was used as a continuous variable. Dependence of mean sheet erosion depth on belowground vegetation and soil properties was modeled with GLMs assuming a gamma distribution as the response variable contained only positive continuous values. The significance of the models was tested using a Type II Wald χ^2 test. Correlations between lateral erosion and soil and vegetation properties in stable samples (only *Atriplex*) could not be explored due to the low sample size ($n = 3$). This method was also applied in Marin-Diaz et al. (2022) to analyze soil stability. All statistical analyses were performed using R 3.5.0 (R Development Core Team, 2022).

3. Results

3.1. Soil and Vegetation Properties in Relation to the Island Morphology

Marsh cores were characterized by a cohesive layer on top of a sandy subsoil, in contrast to dune and bare tidal flat samples, which consisted entirely of sandy profiles (Figure 4). Cohesive layer thickness varied across the island, with the thickest (up to ~28 cm) found in the oldest marsh (>58 years old) with *Atriplex* (Figure 4). Thickness could be related to elevation and marsh age. Older and lower elevated areas connected to the creek (~1.1 m MSL), like the western and oldest part of the marsh, had the thickest cohesive sediment layer (~20 cm) (Figure 4). More elevated areas (~1.4–1.9 m MSL) toward the east (32–58 years old) had thinner cohesive layers (~7–2 cm). The high elevation in this eastern area was not natural but the remnants of a man-made dune ridge. Finally, the youngest marshes in the east near the tidal flats (<32 years), which have been developing during a shorter time period, had thin cohesive layers (~2 cm) despite their low elevation (~1.1 m) (Figure 4).

The cohesive top layer consisted of smaller grain size (<95 μm), higher organic content (>10%), higher soil water content (>40%) and lower bulk density (<1 g cm^{-3}) than the sandy subsoils, the dune and tidal flat locations ($F_{4,10} = 221.7$, $p < 0.001$; $F_{4,10} = 405.4$, $p < 0.001$; $F_{4,10} = 305.4$, $p < 0.001$; $F_{4,10} = 40.6$, $p < 0.001$; respectively) (Figures 5a and 5b). Belowground biomass was higher (>0.1 g cm^{-2}) in the marsh cores compared to the dune cores, with the highest values for *Aster*, followed by *Atriplex* and lastly *Elytrigia* ($F_{4,10} = 52.27$, $p < 0.001$) (Figure 5c). Tidal flat cores did not have any vegetation.

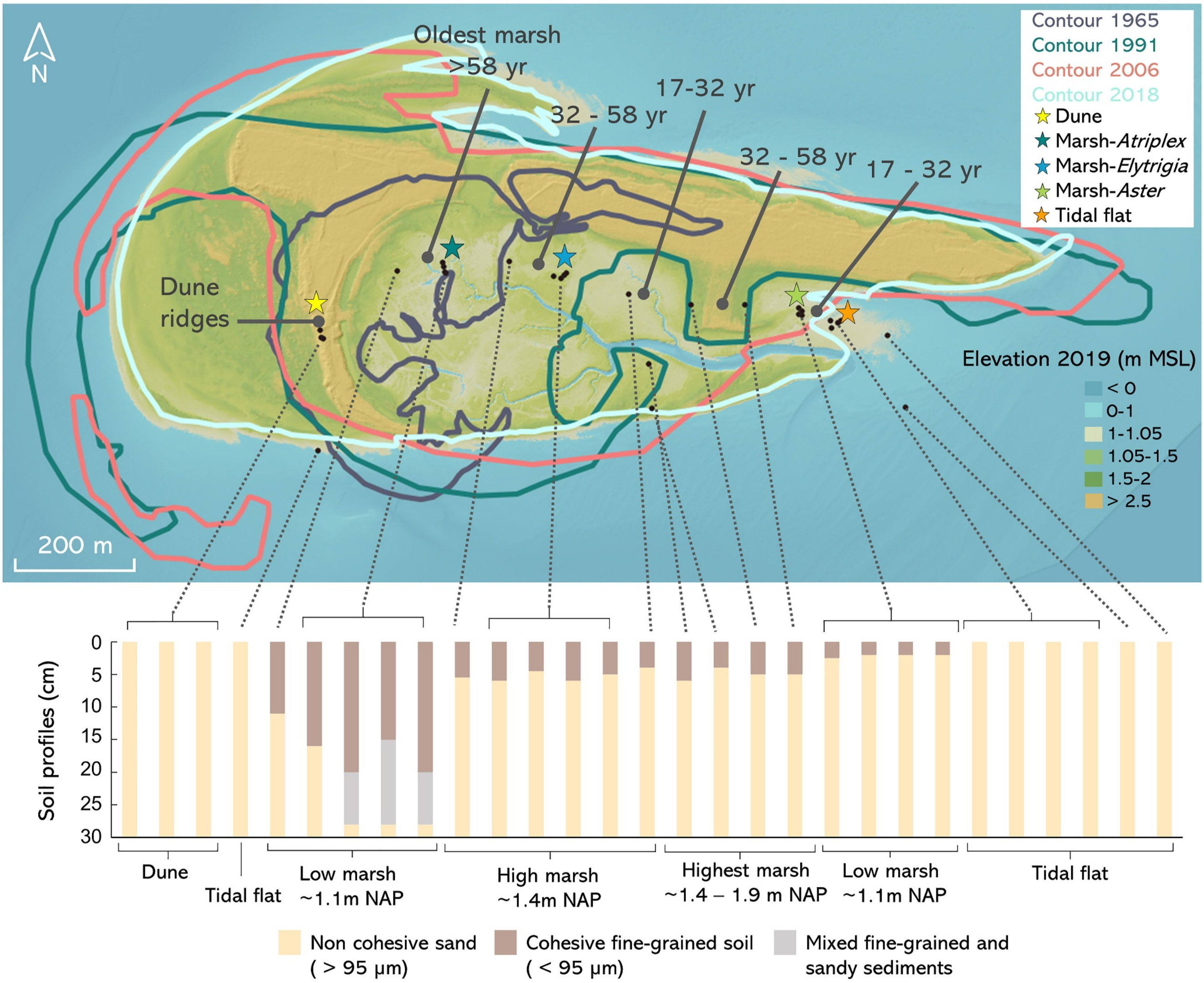

Figure 4. Soil profiles indicating the cohesive topsoil thickness (cm, in brown) measured at different locations across the island (indicated by black dots in the map). Due to the origin of this island, we assumed that deeper layers would be part of the sandy subsoil. Stars indicate the location of the cores used for the erosion tests. Contour lines of the island from 1965, 1991, 2006 and 2018 are shown as a reference for the indicated age of the marsh areas. Digital elevation map from 2019 (source GeoTiles.nl, 1 m resolution).

3.2. Sheet and Lateral Erosion

For sheet erosion tests, most of the erosion occurred within the first 10 min, and for lateral erosion, most occurred within the first hour (Figures 6a and 6b). After that, the sediment was either 100% eroded or eroded at slower rates, erosion increasing by 1.5–2.5 times the values observed at 10 min for sheet erosion and by 1.5–2.5 times the values observed at 1 h for lateral erosion. By the end of the experiments, less than 1 cm of erosion occurred in the resistant samples during the 3-hr sheet erosion test, and less than 20% volume was lost in the resistant samples during the 45-hr lateral erosion test (Figures 6a and 6b).

More specifically, all marsh locations (*Atriplex*, *Elytrigia* and *Aster*) were resistant to sheet erosion independent of cohesive top layer thickness (Figure 6c). The final value of sheet erosion resistance did not differ significantly among marsh locations, with less than 1 cm erosion depth when subtracting the initial debris lost after 10 min (one-way ANOVA: $F_{2,6} = 0.14$, $p > 0.05$) (Figure 6d). In contrast, both the dune and sandflat samples were completely eroded in the first 10 min (Figures 6a and 6b).

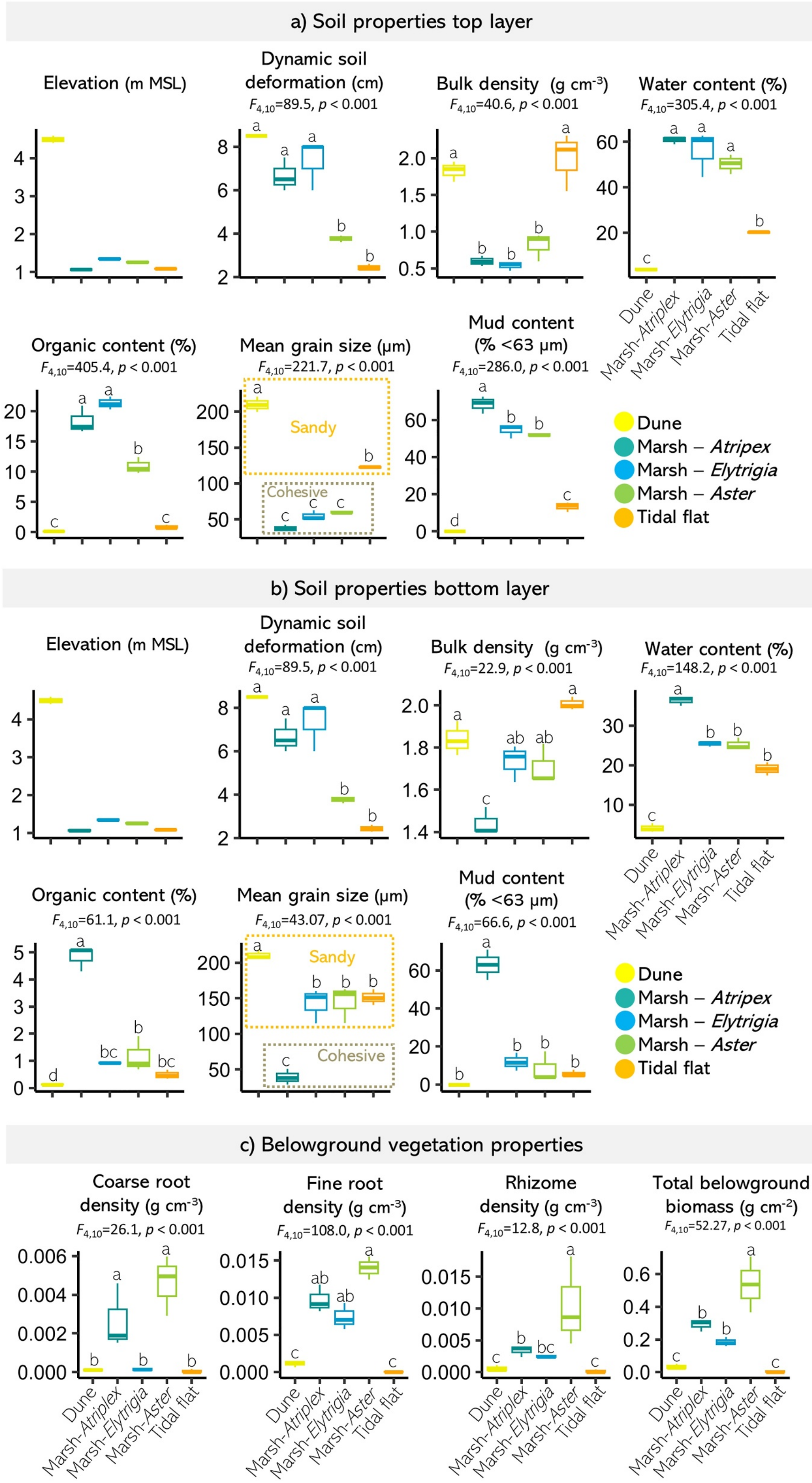

Figure 5. (a) Soil properties from the top layer for each habitat (0–5 cm depth), or to the start of the sandy subsoil in marsh-Aster (~2 cm); (b) soil properties from the bottom layer of the samples, up to 20 cm depth; and (c) vegetation belowground properties from soil samples between 0 and 20 cm depth. ANOVA results for each plot are stated below each variable name. Significant differences between habitats are indicated by letters (Tukey HSD, $p < 0.05$).

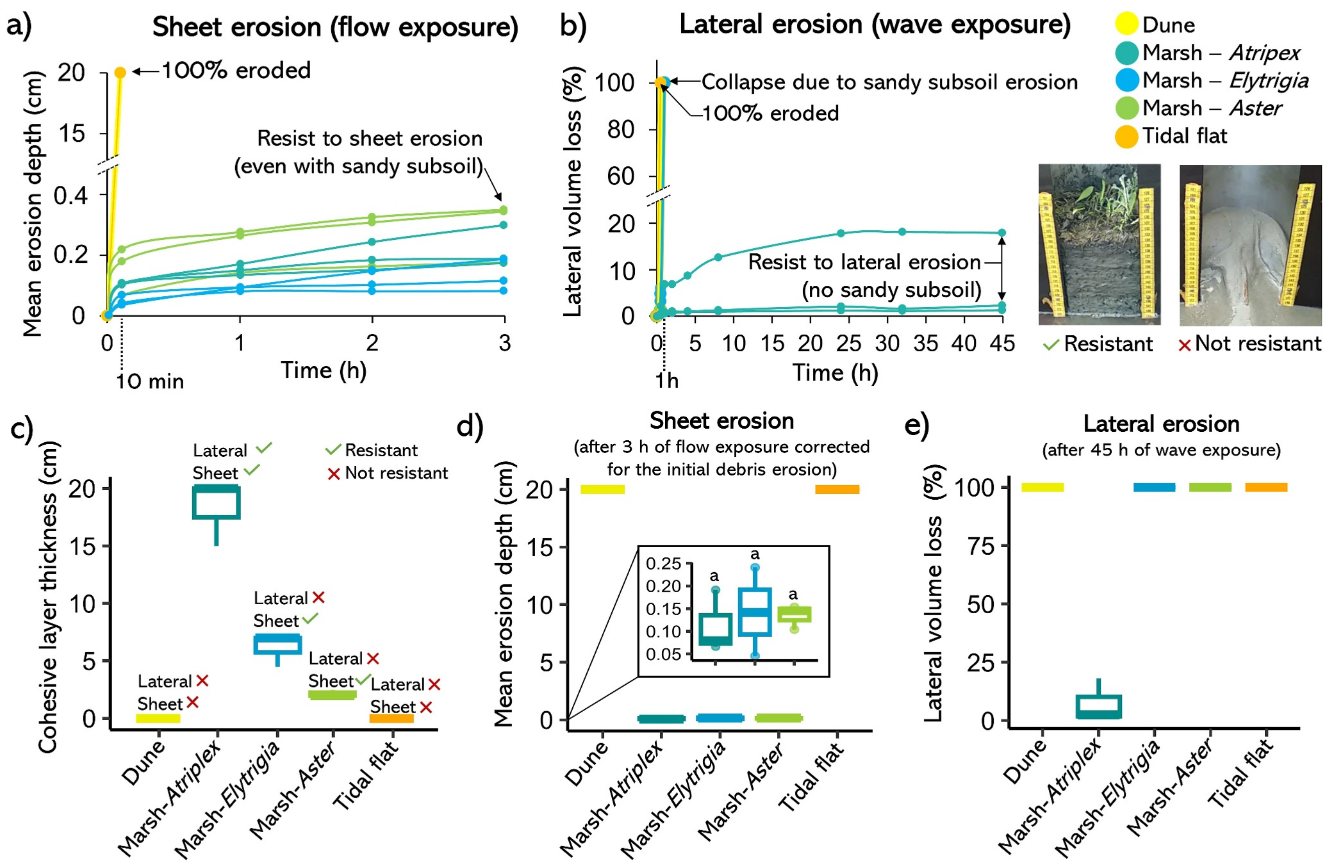

Figure 6. Results of the erosion tests including (a) Sheet erosion over time measured as erosion depth (cm); (b) Lateral erosion over time measured as volume loss (%). Images are examples of resistant and not resistant cores after the first minute of wave exposure; (c) Cohesive layer thickness at the different locations and its relationship with sheet and lateral erosion resistance. Not resistant indicates the collapse of the cohesive top layer in marsh samples after the erosion of the sandy subsoil or the 100% soil erosion in dune and tidal flat cores; (d) differences in sheet erosion after the 3-hr erosion test corrected for the initial debris erosion, where 20 cm is complete erosion. In the subplot, letters depict non-significant differences between resistant locations (Tukey HSD, $p > 0.05$); and (e) differences in lateral erosion after the 45-hr erosion test.

Regarding lateral erosion, only the *Atriplex* marsh (>58 years old) with the thickest cohesive layer (>15 cm) resisted, with 1%–18% erosion after 45 hr of wave exposure (Figures 6b and 6c and 6e). The *Elytrigia* (32–58 years old) and *Aster* (17–32 years old) marshes, with thinner cohesive layers (<10 cm), collapsed when the underlying sand layer was eroded, although the cohesive top layer remained relatively intact. Similar to sheet erosion, dune and sandflat cores were completely eroded in the first 5 min after exposure to waves in the flume.

3.3. Relationships Between Environmental Factors, Sheet Erosion, and Lateral Erosion Comparing All the Samples

Resistance to sheet erosion was correlated with both the biotic and abiotic properties of the top layer (from 0 to 5 cm depth) (Figure 7a). Finer sediment (<95 μm), higher total belowground biomass (>0.1 g cm^{-2}), higher root density (>0.005 g cm^{-3}), especially fine root density (>0.005 g cm^{-3}), higher organic content (>10%) and lower bulk density (<1 g cm^{-3}) were significantly correlated with higher sheet erosion resistance (Figure 7a). Moreover, many of these variables were strongly correlated (Figure S1). Coarse root density and soil dynamic deformation were the only variables not correlated with erosion. Lateral erosion was also explained by the same explanatory variables as sheet erosion (Figure 7b). In contrast to sheet erosion, cohesive sediment layer thickness was the most important driver of lateral erosion resistance (Figure 6c).

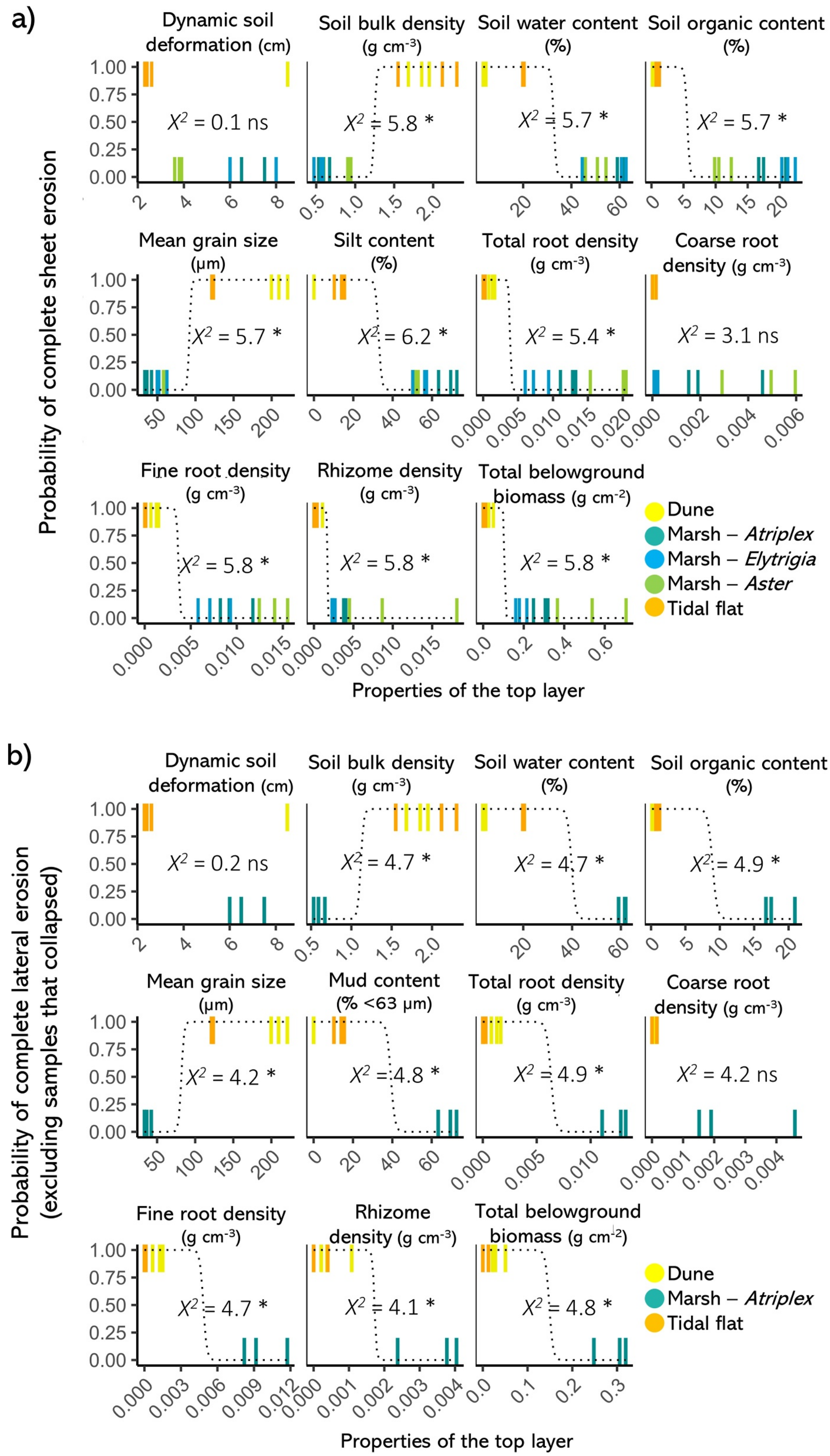

Figure 7. Relationships between (a) sheet erosion after the 3-hr erosion test and the properties of the soil and belowground vegetation; with erosion treated as binomial (either completely eroded or resistant) and (b) lateral erosion after the 45-hr erosion test and the properties of the soil and belowground vegetation; including cores that either completely eroded (dune and tidal flat) or resisted (marsh with *Atriplex*) but excluding cores that collapsed due to thin cohesive layers. Coefficients correspond to logistic regressions. Significance codes refer to $p < 0.01$ (*) and $p > 0.05$ (ns).

3.4. Relationships Between Environmental Factors, Sheet Erosion, and Lateral Erosion Comparing Only Resistant Samples

Within the marsh cores resistant to sheet erosion (*Atriplex*, *Elytrigia*, and *Aster*), none of the vegetation nor soil properties significantly explained the small and non-significant differences (<0.5 cm) in sheet erosion between cores (Figures 6d and 8). Correlations between lateral erosion and soil and vegetation properties in stable samples (only *Atriplex*) could not be explored due to the low sample size (n = 3). However, although anecdotal, we observed that the sample that eroded the most had higher soil dynamic deformation than the other *Atriplex* samples.

4. Discussion

Back-barrier islands are mobile but may disappear due to changes in hydrodynamics and sediment dynamics in a tidal basin (Govers & Reijers, 2021), highlighting the need to understand their soil erosion resistance, particularly in relation to soft engineering measures that are increasingly proposed to guarantee their survival and that of linked ecosystem services (Govers & Reijers, 2021; Sirianni et al., 2022). In this study, we investigated the soil erosion resistance to hydraulic forces of different habitats across a sandy back-barrier island in relation to island development and management. Furthermore, to our knowledge, we present the first experimental comparison between sheet and lateral soil erodibility of sandy habitats under controlled conditions (e.g., references in Brooks et al., 2020; Infantes et al., 2021). Overall, this study demonstrates that lateral and sheet erosion are uncorrelated and that soft engineering measures such as beach nourishment may increase the back-barrier island's soil erosion resistance by creating sheltered conditions for marsh development.

4.1. Erodibility of Soft-Sediment Habitats in a Back-Barrier Island

This study shows, as expected, that the marsh habitats were more resistant to sheet erosion. This was attributed to their cohesive topsoil layer accreted by the marsh vegetation, which is characterized by high belowground biomass - especially high fine root density, high organic content, low bulk density and high mud content compared to the easily erodible sandy soils in the dune and tidal flats. Although the percentage of lateral erosion was not measured for marshes dominated by *Elytrigia* and *Aster* due to their premature collapse, we speculate that the cohesive top layer, with similar properties as the *Atriplex* marsh (Figure 5), would also have been erosion resistant (Marin-Diaz, Govers, et al., 2021; Wang et al., 2017). These properties have been previously related to an increase in the erosion resistance on other types of marshes, both top (Coops et al., 1996; Marin-Diaz et al., 2022; Paul & Kerpen, 2021; Spencer et al., 2016) and laterally (De Battisti et al., 2019; Feagin et al., 2009; Ford et al., 2016; Marin-Diaz, Govers, et al., 2021; Wang et al., 2017).

Nevertheless, this study demonstrates that although marshes on a back-barrier island can have an erosion-resistant topsoil with low erosion rates, which is important during overwash conditions, they may not be resistant to lateral erosion if the subsoils are sandy. These types of profiles are commonly found in barrier islands, where cohesive top layers can form on initially unstable sand flats during back-barrier marsh development (Marin-Diaz, Govers, et al., 2021; Olff et al., 1997) (Figures 2 and 4). Changes in soil properties with depth are thus important to be considered when assessing erosion vulnerability because although some marshes may not be on a cliff at present, they could eventually become laterally exposed on the island edges due to shoreline erosion and/or migration of the dune over the marsh, which can occur relatively fast in migrating islands (Cooper, 2013; Govers & Reijers, 2021). These types of profiles may also be more vulnerable to undercutting at the base of the cliff (Brooks et al., 2020). For instance, the south of Griend had marsh habitat in 2006; however, shoreline retreat can be observed between 2006 and 2018 (Figure 3b). Field observations of the area reveal escarpments, indicating that previously unexposed areas are now vulnerable to hydrodynamic exposure (Figure 9). Finally, it is important to consider that although lateral retreat is most rapid when the subsoil is unconsolidated sand, even cohesive or organic-rich marsh subsoils progressively erode under sustained wave forcing and experience mass failure (Bendoni et al., 2016; Francalanci et al., 2013).

While our results show that erosion resistance was positively related to finer sediments (<95 μm), in a previous study we found that sediment grain size alone may not be a good erosion indicator because there are marshes with coarse sandy soils which are also resistant to sheet erosion due to their high belowground plant biomass and organic content (Marin-Diaz et al., 2022). Therefore, we argue that high belowground biomass, particularly high fine root density, may be a better proxy for erosion resistance. Furthermore, our study primarily focused on the

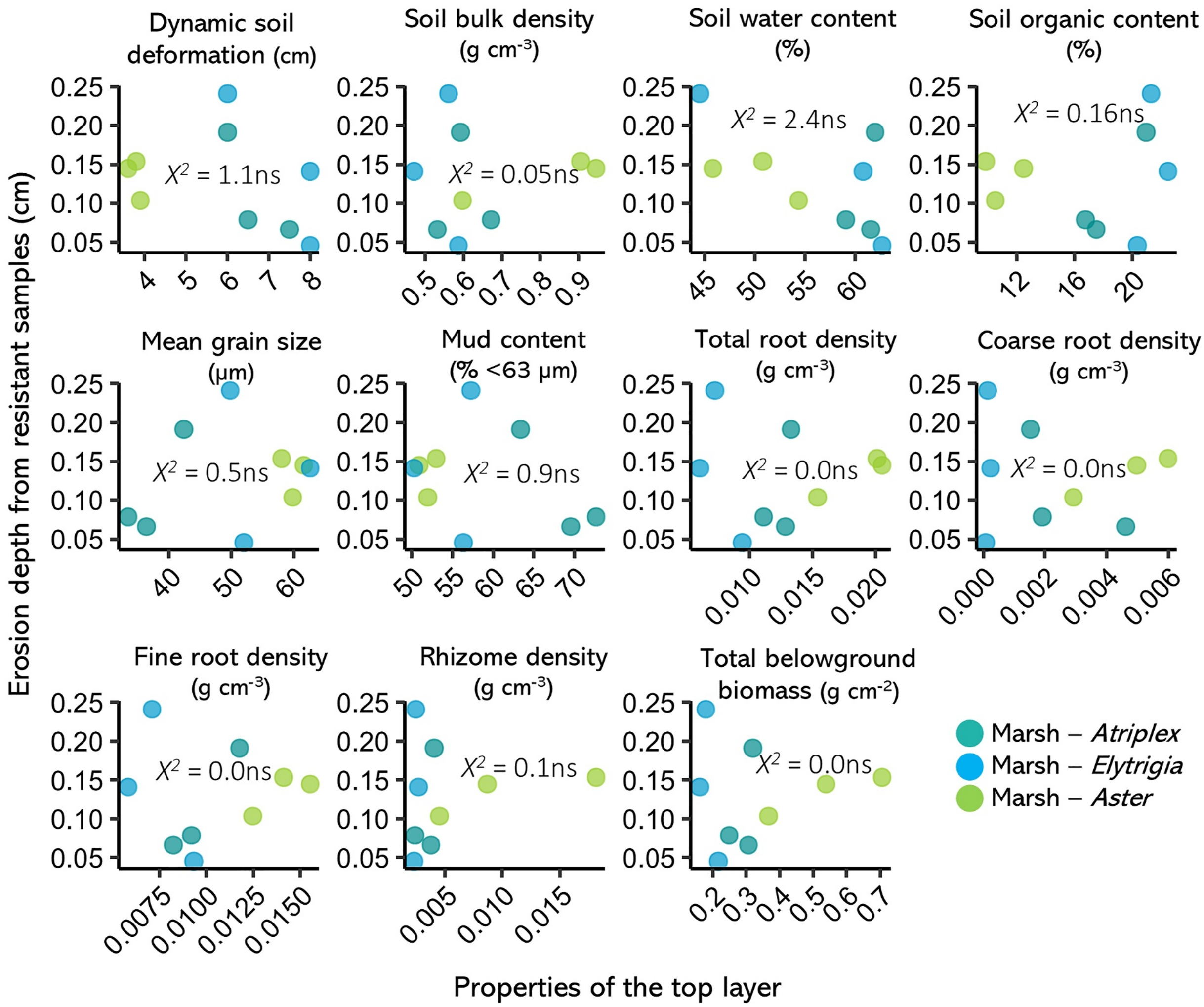

Figure 8. Relationships between sheet erosion after the 3-hr erosion test corrected for the initial debris erosion and the properties of the soil and belowground vegetation, including only cores that resisted the waterflow exposure (marsh with *Atriplex*, *Elytrigia*, and *Aster*). Coefficients correspond to gamma correlations. Significance codes refer to $p > 0.05$ (ns). Note that relationships for the lateral erosion were not performed due to the low sample size of resistant soils (only marsh-*Atriplex*).

intrinsic soil erosion resistance, excluding the effect of the aboveground vegetation. However, it is important to note that coastal vegetation can also reduce erosion by reducing the hydrodynamics within the canopy, thereby lowering shear stress on the soil (Brooks et al., 2020; Feagin et al., 2019; Möller et al., 2014).

Dune ridge vulnerability to hydrodynamics was expected, as this sandy habitat can erode and migrate relatively fast in fetch-limited barrier islands during storms (Coops et al., 1996). The sampled dune vegetation, *A. arenaria*, had less belowground biomass, fine root density and organic content than marsh vegetation, explaining its lower resistance to erosion. However, although our results indicate complete erosion of the dune samples under the selected exposure conditions, dune vegetation still plays an important role in capturing sediment, increasing dune height and reducing deflation (Feagin et al., 2015). These factors are essential for maintaining healthy dunes that in turn will create the sheltered conditions needed for marsh development.

Lastly, while these results provide valuable insights on intrinsic soil erosion rates, it is important to note that they are not generalizable to island-scale erosion rates due to the influence of extrinsic factors on large-scale erosion rates, such as vegetation canopy effects, mass failure processes at the edge (non-linear slumping processes), dune and marsh platform elevation and morphology, or changing hydrodynamic conditions and exposure over time (Brooks et al., 2020; Francalanci et al., 2013; Houser et al., 2008; Priestas et al., 2015; Wang et al., 2017). However, small-scale experiments under controlled conditions are crucial for understanding the intrinsic erosion resistance of soils by eliminating the effect of extrinsic factors in the field, thus providing an approximation of

Figure 9. Examples of marsh soils that have become laterally exposed on the island southern edges.

how different soil types will respond to hydrodynamic exposure. Therefore, further research is warranted to better understand back-barrier island-scale erosion rates.

4.2. Soil Erosion Resistance to Hydraulic Forces of a Back Barrier Island's Habitats in Relation to the Island's Management and Development

The shape and migration of back-barrier islands is dependent on both storm climate and vegetation structure (Cooper et al., 2007; Morton, 2002; Pilkey et al., 2009). Typically, back-barrier islands feature a beach or a chenier ridge on the exposed side formed during strong storm events which provides a sheltered area for marsh formation (McBride et al., 2007; Neal et al., 2002; Pilkey et al., 2009; Sirianni et al., 2022) (Figure 1). However, increased storm surge frequency may lead to insufficient time for islands to recover between floods, reducing marsh development rates and ultimately leading to island losses (Cooper, 2013; Morton, 2002; Timmons et al., 2010; Vinent et al., 2021; Vinent & Moore, 2015). Similarly, a lack of sediment input could negatively affect their accretion and recovery after storms (e.g., Hu et al., 2021; Kirwan et al., 2016; Ladd et al., 2019; Timmons et al., 2010). In the specific case of Griend, there were additional factors promoting erosion, such as human-induced changes in the tidal range after the closing-off of a nearby estuary, which led to increased island losses (Brouwer et al., 1950; Govers & Reijers, 2021). Hence, management interventions may be carried out to ensure the future of these islands and their linked ecosystem services (Brasseur et al., 2015; Govers & Reijers, 2021; Oliver & Ramirez-Avila, 2019; Rosati, 2009).

On Griend, soft-structure coastal engineering, such as the sand dikes constructed in the 1980s, was implemented to facilitate marsh development by creating sheltered conditions (Figures 3a and 3b). By facilitating marsh development and thus the accretion of cohesive topsoils, soft engineering measures can indirectly increase soil erosion resistances of the sheltered side of the island. However, attempts at dune and/or island fixation should be avoided as these can interfere with the natural geomorphic development of the marshes on this type of island (Arens et al., 2013; Govers & Reijers, 2021; Osswald et al., 2019; Timmons et al., 2010). If only sheltered conditions are provided as a result of fixation, adequate flooding regimes through creeks or washovers may cease, resulting in reduced marsh accretion due to a lack of sediment supply. This would hamper a back-barrier island to keep up with sea level rise, increasing the risk of drowning (Koppenaal et al., 2021; Reed et al., 1999).

Constructing areas with lower elevations in the dune or sand ridges to promote washovers, such as the interventions done in 2016 in Griend, may prevent the complete reduction of island dynamics (Govers & Reijers, 2021; Rosati, 2009; Timmons et al., 2010). Other measures may be considered if the sediment input in the marsh is too low, such as mud addition, also known as thin layer placement (Raposa et al., 2023; Rosati, 2009).

The variability in the cohesive topsoil thickness accreted by marshes was linked to marsh age and inundation time (elevation). With increasing age, marshes have more time to trap fine sediment and accumulate more organic matter coming from aboveground and belowground biomass as well as litter, and therefore form thicker cohesive top layers (Bass et al., 2022; Nolte et al., 2013; Nyman et al., 2006; Olff et al., 1997; Van de Koppel et al., 2005). Similarly, marshes that established at intermediate elevation (∼1.1 m MSL in our study site), were more frequently flooded and thus had more opportunities to trap sediment than marshes formed at higher elevations (>1.4 m MSL in our study site). The thickness of the cohesive layer may also depend on the vegetation traits, as some species may produce more biomass, degrade at different rates, or have more canopy roughness and thus enhance sedimentation (Bass et al., 2022; Nolte et al., 2013). However, in this study, it was not possible to disentangle the extent to which the increased thickness of the cohesive top layer was due to differences in vegetation species or the effects of elevation, which influences inundation frequency and species distribution (Bockelmann et al., 2002; Hayden et al., 1995; Olff et al., 1997). Lastly, the creek structure may also influence the thickness of the cohesive topsoil. For instance, in our study, the lower elevated areas connected to flood plains from a creek (i.e., *Atriplex* marsh) were also related to thicker cohesive layers. This could be due to being closer to the creek where higher sediment settlement occurs (Koppenaal et al., 2021; Reed et al., 1999).

Overall, sand-island management aimed at enhancing soil stability provided by coastal vegetation may be important for ensuring long-term resilience of sandy islands and their associated ecological communities, particularly in the face of increasing storm-surges and sea level rise, by promoting the accretion of cohesive marsh soils. Soft engineering measures should consider marsh elevation relative to mean sea level and well-connected creek systems and washovers to allow for some natural dynamics, which are characteristics of back-barrier islands. This study also highlights the importance of simultaneously considering both lateral and sheet erosion when assessing the erosion resistance of sandy habitats. While marshes may appear resistant to sheet erosion, which is important during overwash, they may still be vulnerable to wave attacks on the island edges, especially when the cohesive topsoil is thin.

Conflict of Interest

The authors declare no conflicts of interest relevant to this study.

Data Availability Statement

Data available via Zenodo Repository https://doi.org/10.5281/zenodo.15594543 (Marin-Diaz et al., 2025).

Acknowledgments
This work is part of the Perspectief research programme All-Risk with project number P15-21 project B1 which is (partly) financed by NWO Domain Applied and Engineering Sciences, in collaboration with the following private and public partners: the Dutch Ministry of Infrastructure and Water Management (RWS), Deltares, STOWA, the regional water authority Noorderzijlvest, the regional water authority Vechtstromen, it Fryske Gea, HKV consultants, Natuurmonumenten, waterboard HHNK. LLG was funded by NWO VENI Grant 016.Veni.181.087 and VCR by NWO VENI Grant VI.Veni.212.059. In addition, we would like to thank Lennart van IJzerloo from the NIOZ for technical assistance, Jantsje van Loon-Steensma from the University of Wageningen for supporting L.M., and Sien and Saar Niermeijer and Jouke van der Meulen who have hosted us on the Ambulant. We are also grateful to the nature managers of Natuurmonumenten and the province of Fryslân for providing access to Griend.

References

Arens, S. M., Mulder, J. P. M., Slings, Q. L., Geelen, L. H. W. T., & Damsma, P. (2013). Dynamic dune management, integrating objectives of nature development and coastal safety: Examples from The Netherlands. *Geomorphology*, *199*, 205–213. https://doi.org/10.1016/j.geomorph.2012.10.034

Bass, J., Granse, D., Hache, I., Jensen, K., Karius, V., Minden, V., et al. (2022). Plant traits affect vertical accretion of salt marshes. *Estuarine, Coastal and Shelf Science*, *276*, 108010. https://doi.org/10.1016/j.ecss.2022.108010

Bendoni, M., Mel, R., Solari, L., Lanzoni, S., Francalanci, S., Oumeraci, H., & Department (2016). Insights into lateral marsh retreat mechanism through localized field measurements. *Water Resources Research*, *52*(2), 1446–1464. https://doi.org/10.1002/2015WR017966.Received

Bockelmann, A. C., Bakker, J. P., Neuhaus, R., & Lage, J. (2002). The relation between vegetation zonation, elevation and inundation frequency in a Wadden Sea salt marsh. *Aquatic Botany*, *73*(3), 211–221. https://doi.org/10.1016/S0304-3770(02)00022-0

Brasseur, S., de Groot, A., Aarts, G., Dijkman, E., & Kirkwood, R. (2015). *Pupping habitat of grey seals in the Dutch Wadden Sea*. Wageningen. Retrieved from http://library.wur.nl/WebQuery/wurpubs/fulltext/362934

Brooks, H., Möller, I., Carr, S., Chirol, C., Christie, E., Evans, B., et al. (2020). Resistance of salt marsh substrates to near-instantaneous hydrodynamic forcing. *Earth Surface Processes and Landforms*, *46*(1), 67–88. https://doi.org/10.1002/esp.4912

Brouwer, G. A., van Dieren, J., Feekes, W., Harmsen, G. W., ten Houten, J. G., Kabos, W. J., et al. (1950). *Griend. Het vogeleiland in de lladdenzee*. Martinus Nijhoff,'s-Gravenhage.

Castagno, K. A., Jiménez-Robles, A. M., Donnelly, J. P., Wiberg, P. L., Fenster, M. S., & Fagherazzi, S. (2018). Intense storms increase the stability of tidal bays. *Geophysical Research Letters*, *45*(11), 5491–5500. https://doi.org/10.1029/2018GL078208

Conery, I., Walsh, J. P., & Reide Corbett, D. (2018). Hurricane overwash and decadal-scale evolution of a narrowing Barrier Island, Ocracoke Island, NC. *Estuaries and Coasts*, *41*(6), 1626–1642. https://doi.org/10.1007/s12237-018-0374-y

Cooper, J. A., Pilkey, O. H., & Lewis, D. A. (2007). Islands behind islands: An unappreciated coastal land form category. In *SI 50 (Proceedings of the 9th international coastal symposium)* (pp. 907–911). Journal of Coastal Research.

Cooper, J. A. G. (2013). Mesoscale geomorphic change on low energy barrier islands in Chesapeake Bay, U.S.A. *Geomorphology*, *199*, 82–94. https://doi.org/10.1016/j.geomorph.2012.06.019

Coops, H., Verheij, H. J., Boeters, R., & van der Velde, G. (1996). Interactions between waves, bank erosion and emergent vegetation: An experimental study in a wave tank. *Aquatic Botany*, *53*(3–4), 187–198. https://doi.org/10.1016/0304-3770(96)01027-3

De Battisti, D., Fowler, M. S., Jenkins, S. R., Skov, M. W., Rossi, M., Bouma, T. J., et al. (2019). Intraspecific root trait variability along environmental gradients affects salt marsh resistance to lateral erosion. *Frontiers in Ecology and Evolution*, *7*, 150. https://doi.org/10.3389/fevo.2019.00150

De Battisti, D., Griffin, J. N., Park, S., & Sa, S. (2020). Below-ground biomass of plants, with a key contribution of buried shoots, increases foredune resistance to wave swash. *Annals of Botany*, *125*, 325–333. https://doi.org/10.1093/aob/mcz125

Elschot, K., Bakker, J. P., Temmerman, S., Van De Koppel, J., & Bouma, T. J. (2015). Ecosystem engineering by large grazers enhances carbon stocks in a tidal salt marsh. *Marine Ecology Progress Series*, *537*, 9–21. https://doi.org/10.3354/meps11447

Feagin, R. A., Figlus, J., Zinnert, J. C., Sigren, J., Martínez, M. L., Silva, R., et al. (2015). Going with the flow or against the grain? The promise of vegetation for protecting beaches, dunes, and barrier islands from erosion. *Frontiers in Ecology and the Environment*, *13*(4), 203–210. https://doi.org/10.1890/140218

Feagin, R. A., Furman, M., Salgado, K., Martinez, M. L., Innocenti, R. A., Eubanks, K., et al. (2019). The role of beach and sand dune vegetation in mediating wave run up erosion. *Estuarine, Coastal and Shelf Science*, *219*(September 2018), 97–106. https://doi.org/10.1016/j.ecss.2019.01.018

Feagin, R. A., Lozada-Bernard, S. M., Ravens, T. M., Mo, I., Yeager, K. M., & Baird, A. H. (2009). Does vegetation prevent wave erosion of salt marsh edges? *PNAS*, *106*(25), 10109–10113. https://doi.org/10.1073/pnas.0901297106

Ford, H., Garbutt, A., Ladd, C., Malarkey, J., & Skov, M. W. (2016). Soil stabilization linked to plant diversity and environmental context in coastal wetlands. *Journal of Vegetation Science*, *27*(2), 259–268. https://doi.org/10.1111/jvs.12367

Francalanci, S., Bendoni, M., Rinaldi, M., & Solari, L. (2013). Geomorphology Ecomorphodynamic evolution of salt marshes: Experimental observations of bank retreat processes. *Geomorphology*, *195*, 53–65. https://doi.org/10.1016/j.geomorph.2013.04.026

Gelman, A., Jakulin, A., Pittau, M. G., & Su, Y. S. (2008). A weakly informative default prior distribution for logistic and other regression models. *Annals of Applied Statistics*, *2*(4), 1360–1383. https://doi.org/10.1214/08-AOAS191

Govers, L. L., & Reijers, V. C. (2021). *Griend: Een bewogen eiland*. KNNV Uitgeverij.

Hayden, B. P., Santos, M. C. F. V., Shao, G., & Kochel, R. C. (1995). Geomorphological controls on coastal vegetation at the Virginia Coast Reserve. *Geomorphology*, *13*(1–4), 283–300. https://doi.org/10.1016/0169-555X(95)00032-Z

Houser, C., Hapke, C., & Hamilton, S. (2008). Controls on coastal dune morphology, shoreline erosion and barrier island response to extreme storms. *Geomorphology*, *100*(3–4), 223–240. https://doi.org/10.1016/j.geomorph.2007.12.007

Howison, R. A., Olff, H., Steever, R., & Smit, C. (2015). Large herbivores change the direction of interactions within plant communities along a salt marsh stress gradient. *Journal of Vegetation Science*, *26*(6), 1159–1170. https://doi.org/10.1111/jvs.12317

Hu, Z., Borsje, B. W., Belzen, J. V., Willemsen, P. W. J. M., Wang, H., Peng, Y., et al. (2021). Mechanistic modelling of marsh seedling establishment provides a positive outlook for coastal wetland restoration under global climate change. *Geophysical Research Letters*, *48*(22), 1–19. https://doi.org/10.1029/2021GL095596

Infantes, E., Smit, J. C. D., Tamarit, E., & Bouma, T. J. (2021). Making realistic wave climates in low-cost wave mesocosms: A new tool for experimental ecology and biogeomorphology. *Limnology and Oceanography: Methods*, *19*(5), 317–330. https://doi.org/10.1002/lom3.10425

Kirwan, M. L., Temmerman, S., Skeehan, E. E., Guntenspergen, G. R., & Fagherazzi, S. (2016). Overestimation of marsh vulnerability to sea level rise. *Nature Climate Change*, *6*(3), 253–260. https://doi.org/10.1038/nclimate2909

Koppenaal, P., Esselink, E. C., van Duin, W. E., & Bakker, J. P. (2021). Temporal and spatial accretion patterns and the impact of livestock grazing in a restored coastal salt marsh. *Estuaries and Coasts*, *45*(2), 510–522. https://doi.org/10.1007/s12237-021-00963-w

Ladd, C. J. T., Duggan-Edwards, M. F., Bouma, T. J., Pagès, J. F., & Skov, M. W. (2019). Sediment supply explains long-term and large-scale patterns in salt marsh lateral expansion and erosion. *Geophysical Research Letters*, *46*(20), 11178–11187. https://doi.org/10.1029/2019GL083315

Leonardi, N., Carnacina, I., Donatelli, C., Ganju, N. K., Plater, A. J., Schuerch, M., & Temmerman, S. (2018). Dynamic interactions between coastal storms and salt marshes: A review. *Geomorphology*, *301*, 92–107. https://doi.org/10.1016/j.geomorph.2017.11.001

Lo, V. B., Bouma, T. J., van Belzen, J., Van Colen, C., & Airoldi, L. (2017). Interactive effects of vegetation and sediment properties on erosion of salt marshes in the Northern Adriatic Sea. *Marine Environmental Research*, *131*, 32–42. https://doi.org/10.1016/j.marenvres.2017.09.006

Loonstra, A. H. J., Piersma, T., & Reneerkens, J. (2016). Staging duration and passage population size of sanderlings in the western Dutch Wadden Sea. *Ardea*, *104*(1), 49–61. https://doi.org/10.5253/arde.v104i1.a4

Marin-Diaz, B., Fivash, G. S., Nauta, J., Temmink, R. J. M., Hijner, N., Reijers, V. C., et al. (2021). On the use of large-scale biodegradable artificial reefs for intertidal foreshore stabilization. *Ecological Engineering*, *170*, 106354. https://doi.org/10.1016/j.ecoleng.2021.106354

Marin-Diaz, B., Govers, L. L., van der Wal, D., Olff, H., & Bouma, T. J. (2021). How grazing management can maximize erosion resistance of salt marshes. *Journal of Applied Ecology*, *58*(7), 1533–1544. https://doi.org/10.1111/1365-2664.13888

Marin-Diaz, B., Govers, L. L., van der Wal, D., Olff, H., & Bouma, T. J. (2022). The importance of marshes providing soil stabilization to resist fast-flow erosion in case of a dike breach. *Ecological Applications*, *32*(6), e2622. https://doi.org/10.1002/eap.2622

Marin-Diaz, B., Reijers, V., Meijer, L., van der Wal, D., Olff, H., Bouma, T., & Govers, L. (2025). Data underlying the publication: "Quantifying soil resistance to sheet and lateral erosion across different habitats on a managed sandy back-barrier island" [Dataset]. *Zenodo*. https://doi.org/10.5281/zenodo.15594543

McBride, R. A., Taylor, M. J., & Byrnes, M. R. (2007). Coastal morphodynamics and Chenier-Plain evolution in southwestern Louisiana, USA: A geomorphic model. *Geomorphology*, *88*(3–4), 367–422. https://doi.org/10.1016/j.geomorph.2006.11.013

Möller, I., Kudella, M., Rupprecht, F., Spencer, T., Paul, M., van Wesenbeeck, B. K., et al. (2014). Wave attenuation over coastal salt marshes under storm surge conditions. *Nature Geoscience*, *7*(10), 727–731. https://doi.org/10.1038/ngeo2251

Morton, R. A. (2002). Factors controlling storm impacts on coastal barriers and beaches - A preliminary basis for near real-time forecasting. *Journal of Coastal Research*, *18*(3), 486–501.

Neal, A., Richards, J., & Pye, K. (2002). Structure and development of shell Chenier's in Essex, southeast England, investigated using high-frequency ground-penetrating radar. *Marine Geology*, *185*(3–4), 435–469. https://doi.org/10.1016/S0025-3227(01)00239-0

Nieuwhof, S., Herman, P. M. J., Dankers, N., Troost, K., & Van Der Wal, D. (2015). Remote sensing of epibenthic shellfish using synthetic aperture radar satellite imagery. *Remote Sensing*, *7*(4), 3710–3734. https://doi.org/10.3390/rs70403710

Nolte, S., Koppenaal, E. C., Esselink, P., Dijkema, K. S., Schuerch, M., De Groot, A. V., et al. (2013). Measuring sedimentation in tidal marshes: A review on methods and their applicability in biogeomorphological studies. *Journal of Coastal Conservation*, *17*(3), 301–325. https://doi.org/10.1007/s11852-013-0238-3

Nordstrom, K. F., & Jackson, N. L. (2012). Physical processes and landforms on beaches in short fetch environments in estuaries, small lakes and reservoirs: A review. *Earth-Science Reviews*, *111*(1–2), 232–247. https://doi.org/10.1016/j.earscirev.2011.12.004
Nyman, J. A., Walters, R. J., Delaune, R. D., & Patrick, W. H. (2006). Marsh vertical accretion via vegetative growth. *Estuarine, Coastal and Shelf Science*, *69*(3–4), 370–380. https://doi.org/10.1016/j.ecss.2006.05.041
Oertel, G. F. (1985). The barrier island system. *Marine Geology*, *63*(1–4), 1–18. https://doi.org/10.1016/0025-3227(85)90077-5
Olff, H., Leeuw, J. D., Bakker, J. P., Platerink, R. J., & van Wijnen, H. J. (1997). Vegetation succession and herbivory in a salt marsh: Changes induced by sea level rise and silt deposition along an elevational gradient. *Journal of Ecology*, *85*(6), 799. https://doi.org/10.2307/2960603
Oliver, B., & Ramirez-Avila, J. J. (2019). Barrier island restoration: A literature review. *World Environmental and Water Resources Congress*, *2019*, 310–319. https://doi.org/10.1061/9780784482353.029
Osswald, F., Dolch, T., & Reise, K. (2019). Remobilizing stabilized island dunes for keeping up with sea level rise? *Journal of Coastal Conservation*, *23*(3), 675–687. https://doi.org/10.1007/s11852-019-00697-9
Otvos, E. G. (2020). Coastal barriers - Fresh look at origins, nomenclature and classification issues. *Geomorphology*, *355*, 107000. https://doi.org/10.1016/j.geomorph.2019.107000
Paul, M., & Kerpen, N. B. (2021). Erosion protection by winter state of salt marsh vegetation. *Journal of Ecohydraulics*, *7*(2), 144–153. https://doi.org/10.1080/24705357.2021.1938252
Piersma, T., Hoekstra, R., Dekinga, A., Koolhaas, A., Wolf, P., Battley, P., & Wiersma, P. (1993). Scale and intensity of intertidal habitat use by knots Calidris canutus in the Western Wadden Sea in relation to food, friends and foes. *Netherlands Journal of Sea Research*, *31*(4), 331–357. https://doi.org/10.1016/0077-7579(93)90052-T
Pilkey, O. H., Cooper, J. A. G., & Lewis, D. A. (2009). Global distribution and geomorphology of fetch-limited barrier islands. *Journal of Coastal Research*, *25*(4), 819–837. https://doi.org/10.2112/08-1023.1
Priestas, A. M., Mariotti, G., Leonardi, N., & Fagherazzi, S. (2015). Coupled wave energy and erosion dynamics along a salt marsh boundary, Hog Island Bay, Virginia, USA. *Marine Science and Engineering*, *3*(3), 1041–1065. https://doi.org/10.3390/jmse3031041
R Development Core Team. (2022). R: A language and environment for statistical computing. Retrieved from https://www.r-project.org/
Raposa, K. B., Woolfolk, A., Endris, C. A., Fountain, M. C., Moore, G., Tyrrell, M., et al. (2023). Evaluating thin-layer sediment placement as a tool for enhancing tidal marsh resilience: A coordinated experiment across eight US national estuarine research reserves. *Estuaries and Coasts*, *46*(3), 595–615. https://doi.org/10.1007/s12237-022-01161-y
Reed, D. J., Spencer, T., Murray, A. L., French, J. R., & Leonard, L. (1999). Marsh surface sediment deposition and the role of tidal creeks: Implications for created and managed coastal marshes. *Journal of Coastal Conservation*, *5*(1), 81–90. https://doi.org/10.1007/BF02802742
Rietveld, C. F. W. (1962). The natural development of the Wadden Sea after the enclosure of the Zuider Sea. *Coastal Engineering Proceedings*, *8*, 42. https://doi.org/10.9753/icce.v8.42
Rosati, J. D. (2009). *Concepts for functional restoration of Barrier Islands*. US Army Corps of Engineers.
RWS. (2013). *Report: Kenmerkende waarden. Getijgebied 2011.0*. Ministerie van Infrastructuur en Milieu, Rijkswaterstaat Centrale Informatievoorziening. Retrieved from https://puc.overheid.nl/rijkswaterstaat/doc/PUC_159573_31/
Seneviratne, S. I., Zhang, X., Adnan, M., Badi, W., Dereczynski, C., Di Luca, A., et al. (2021). Weather and climate extreme events in a changing climate. In *Climate change 2021: The physical science basis. Contribution of working group I to the sixth assessment report of the intergovernmental panel on climate change*. https://doi.org/10.1017/9781009157896.013
Sirianni, H., Sirianni, M. J., Mallinson, D. J., Lindquist, N. L., Valdes-Weaver, L. M., Moody, M., et al. (2022). Quantifying recent storm-induced change on a small fetch-limited barrier island along North Carolina's crystal coast using aerial imagery and LiDAR. *Coasts*, *2*(4), 302–322. https://doi.org/10.3390/coasts2040015
Spencer, T., Möller, I., Rupprecht, F., Bouma, T. J., van Wesenbeeck, B. K., Kudella, M., et al. (2016). Salt marsh surface survives true-to-scale simulated storm surges. *Earth Surface Processes and Landforms*, *41*(4), 543–552. https://doi.org/10.1002/esp.3867
Timmons, E. A., Rodriguez, A. B., Mattheus, C. R., & DeWitt, R. (2010). Transition of a regressive to a transgressive barrier island due to back-barrier erosion, increased storminess, and low sediment supply: Bogue Banks, North Carolina, USA. *Marine Geology*, *278*(1–4), 100–114. https://doi.org/10.1016/j.margeo.2010.09.006
Van Rijn, L. C. (1984a). Sediment transport, Part II: Suspended load Transport. *Journal of Hydraulic Engineering-ASCE*, *110*(11), 655–664. https://doi.org/10.1061/(ASCE)0733-9429(1984)110:11(1613)
Van de Koppel, J., Van der Wal, D., Bakker, J. P., & Herman, P. M. J. (2005). Self-organization and vegetation collapse in salt marsh ecosystems. *The American Naturalist*, *165*(1), 1–12. https://doi.org/10.1086/426602
Van Rijn, L. C. (1984b). Sediment transport, Part I: Bed load transport. *Journal of Hydraulic Engineering–ASCE*, *110*(10), 1431–1456. https://doi.org/10.1061/(ASCE)0733-9429(1987)113:9(1187)
Vinent, O. D., & Moore, L. J. (2015). Barrier island bistability induced by biophysical interactions. *Nature Climate Change*, *5*(2), 158–162. https://doi.org/10.1038/nclimate2474
Vinent, O. D., Schaffer, B. E., & Rodriguez-Iturbe, I. (2021). Stochastic dynamics of barrier island elevation. *Proceedings of the National Academy of Sciences of the United States of America*, *118*(1), 6–11. https://doi.org/10.1073/pnas.2013349118
Wang, H., van der Wal, D., Li, X., van Belzen, J., Herman, P. M. J., Hu, Z., et al. (2017). Zooming in and out: Scale-dependence of extrinsic and intrinsic factors affecting salt marsh erosion. *Journal of Geophysical Research: Earth Surface*, *122*(7), 1455–1470. https://doi.org/10.1002/2016JF004193